Engineering and Computational Mechanics
Volume 165 Issue EM4
Radial jet due to plume impingement on a horizontal surface
Rooney and Linden
ice | proceedings

Proceedings of the Institution of Civil Engineers
Engineering and Computational Mechanics 165 December 2012 Issue EM4
Pages 223–233 http://dx.doi.org/10.1680/eacm.11.00010
Paper 1100010
Received 27/05/2011 Accepted 19/09/2011
Published online 02/08/2012
Keywords: fire engineering/fluid mechanics/mathematical modelling

ice
Institution of Civil Engineers
publishing

Radial jet due to plume impingement on a horizontal surface

Gabriel G. Rooney PhD
Senior Scientist, Met Office, Fitzroy Road, Exeter, UK

Paul F. Linden FRS
GI Taylor Professor of Fluid Mechanics, Department of Applied Mathematics and Theoretical Physics, University of Cambridge Centre for Mathematical Sciences, Cambridge, UK

Results of a theoretical and experimental investigation into the properties of a thermal impingement current are presented. The current is generated by a plume from a fire impinging on a horizontal ceiling. Axisymmetric plume and gravity-current similarity solutions are used to relate the current velocity, depth and temperature to the fire strength and ceiling height, and to discuss the convective heat transfer to the ceiling. Experimental results of current temperature and heat transfer to the ceiling are used to verify the model, showing how the heat transfer scales with the similarity velocity and temperature difference.

Notation

A	dimensionless scaling in turbulent shear relation
b	plume radius
C_P	specific heat capacity of air
c_1	dimensionless constant
c_2	dimensionless constant
d_N	jet nozzle diameter
E	scaling factor in laminar heat flux relation
F	exponent in laminar heat flux relation
F_0	initial buoyancy flux of buoyant jet
F_c	ceiling-jet buoyancy flux
F_p	plume buoyancy flux
Fr	Froude number
f	reduction rate of buoyancy flux per unit impingement area
f_1	function of dimensionless radius that modifies ceiling-jet velocity
f_2	function of dimensionless radius that modifies ceiling-jet depth
f_3	function of dimensionless radius that modifies ceiling-jet reduced gravity
$\boldsymbol{g}$	acceleration due to gravity
$\boldsymbol{g}'_c$	ceiling-jet reduced gravity
$\boldsymbol{g}'_p$	plume reduced gravity
H	ceiling height
h	ceiling-jet depth
k	thermal conductivity
l_M	jet length (scaling parameter for buoyant jet)
M	jet momentum flux
M_0	initial momentum flux of buoyant jet
N	buoyancy frequency
Nu	Nusselt number
Pr	Prandtl number
$\dot{Q}$	convective power of fire
Q^*	dimensionless convective power of fire
$\dot{q}$	turbulent heat flux
$\dot{q}_j$	turbulent heat flux (jet)
$\dot{q}_{lam}$	laminar heat flux
$\dot{q}_p$	turbulent heat flux (plume)
R	ratio of maximum to similarity-scale ceiling-jet properties
Ra	Rayleigh number
Re	Reynolds number
Ri	Richardson number
r	radial coordinate
$\tilde{r}$	dimensionless radial coordinate
T	ambient temperature
u	ceiling-jet velocity
u^*	dimensionless ceiling-jet velocity
u_m	maximum ceiling-jet velocity
V_c	ceiling-jet volume flux
V_p	plume volume flux
v_e	centreline velocity of laminar flow
w	plume velocity
z	vertical coordinate
α	plume entrainment constant
β	thermal expansion coefficient
ΔT	current/ambient temperature difference
ΔT^*	dimensionless current/ambient temperature difference
ΔT_m	maximum current/ambient temperature difference
ΔT_s	current/ceiling surface temperature difference
ν	kinematic viscosity
π	circumference/diameter ratio of a circle
ρ	ambient density
φ	jet heat-flux enhancement factor

1. Introduction

The impingement of a plume or jet on a flat surface is a common occurrence and studies of this type of flow have been made for a variety of applications. It has been considered for the cases of laminar, turbulent and supersonic flow, for surfaces either normal or at an angle to the flow direction, for isothermal flow and for heat-exchanging situations involving either a heated surface or a heated stream of fluid (e.g. Beyler, 1986; Carling and Hunt, 1974; Donaldson *et al.*, 1971; Kataoka *et al.*, 1987; Stevens and Webb, 1991; Watson, 1964; Yao and Marshall, 2007).

The case of a turbulent, buoyant fluid (referred to as a plume) arising from a source of small extent compared to the flow dimensions and impinging normally onto a horizontal surface is discussed in this paper. This encompasses both a hot fluid travelling upwards and a negatively buoyant (cold) fluid travelling downwards. The model is thus applicable to the modelling of fire dynamics, as well as to a range of situations in the atmosphere and ocean. The flow may be divided into four regions

- the plume source
- the vertical plume flow
- the impingement region
- the impingement current flowing out of that region.

For positively buoyant flow such as that from a fire, the flat surface is the ceiling of the domain and the terms impingement current and ceiling jet are interchangeable.

The present study combines two results that have been obtained separately, namely similarity models of a plume and of a radial gravity current. The first of these flows has been studied extensively and the second less so, although it has clear application to the impingement current. The combination of the two is found to produce the scaling dependence of ceiling jets (from fires) on convective fire strength and ceiling height, which has been found useful in the past when analysing experimental results. The flow and heat transfer in the impingement region is also re-examined in an attempt to unify previous results obtained in the cases of fire plume and jet flow. The model derived is verified and extended with the aid of the experimental results.

2. Theoretical model

The steady-state case will be considered. This may be assumed to apply immediately following the passage of the front of impinging fluid through the ceiling area of interest. For a ceiling jet that loses heat to the ceiling by conduction, in the initial period following passage of the front it may also be assumed that the ceiling and ambient temperatures are equal (or similar); this permits some simplifications in modelling. The duration of this initial period will depend on the thermal inertia of the ceiling material. At longer times, heat transfer to the ceiling will reduce the temperature difference and conductive losses from the ceiling jet will then be reduced. Figure 1 shows a diagram of the flow configuration to be analysed.

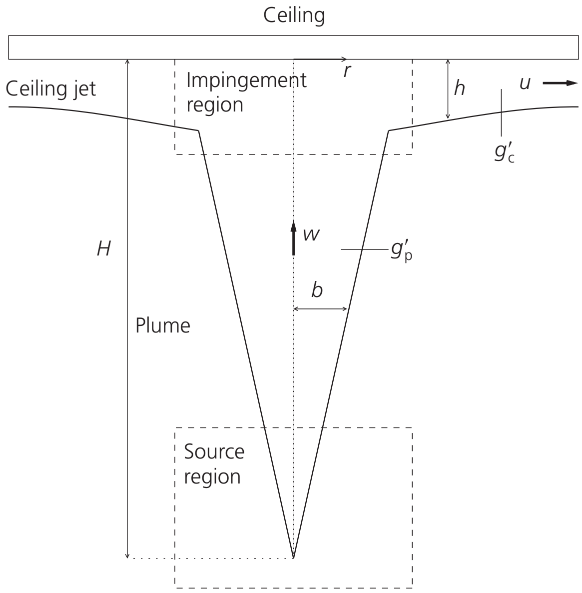

Figure 1. Diagram of the flow under discussion

2.1 Plume

The theoretical model for an axisymmetric plume is, in many aspects, already well-established. In general, the use of a pure-plume similarity model (i.e. a model of a plume arising from a point source of buoyancy only) is appropriate beyond a near-source region that has a length scale set by the properties of the source. In some cases, a virtual origin (i.e. a pure-plume source at some vertical displacement from the actual source) may be used to match the flow properties to the similarity model.

For the particular case of a fire plume, additional near-source effects must be considered; namely, the generation of the plume buoyancy flux through combustion and the large (non-Boussinesq) density contrast caused by the high temperatures within and above the combusting zone. In effect, these additional features provide further constraints on the near-source length scale. However, it may be shown (Rooney, 1997) that, above the visible-flame region, the usual Boussinesq plume similarity solution is adequate for the description of a fire plume. This solution will therefore be used to model the plume in the following analysis.

For a plume with a buoyancy flux F_p, the representative values of the vertical velocity w, radius b and reduced gravity g'_p at a height H above the source (in an unstratified ambient) are, respectively (e.g. Devenish *et al.*, 2010; Turner, 1973)

1a. $$w = \frac{5}{6\alpha\pi^{1/3}}\left(\frac{9\alpha}{10}\right)^{1/3} F_p^{1/3} H^{1/3}$$

1b. $$b = \frac{6\alpha}{5} H$$

1c. $$g'_{\mathrm{p}} = \frac{5}{6\alpha\pi^{2/3}} \left(\frac{9\alpha}{10}\right)^{-1/3} F_{\mathrm{p}}^{2/3} H^{-5/3}$$

where $\alpha \approx 0{\cdot}1$ is the plume entrainment constant and the subscript p has been introduced to distinguish plume variables from ceiling-jet variables to be introduced later. The constant buoyancy flux $F_{\mathrm{p}} = \pi b^2 w g'_{\mathrm{p}}$ is related to the convective power output $\dot{Q}$ of the plume source by (e.g. Hunt and Linden, 2001)

2. $$F_{\mathrm{p}} = \frac{g\beta\dot{Q}}{\rho C_{\mathrm{P}}}$$

(see Table 1 for a statement of the other quantities in this expression). The convective power output of a fire is usually a large proportion (e.g. 70%) of the total power of combustion, with the remainder being lost through radiative processes (Drysdale, 1985; Tamanini, 1977).

2.2 Ceiling jet

When the plume domain is bounded by a horizontal ceiling at height H above the source, the plume will impinge on the ceiling and spread out radially as a ceiling jet. The two-dimensional (2D) ceiling jet has been described (e.g. Emmons, 1991). However, for the case of a localised fire in a large enclosure, the appropriate description of the flow is as an axisymmetric ceiling jet, which has different features from those of the 2D case.

It is useful to begin the analysis by considering the case without thermal exchange between the ceiling jet and the ceiling. This is equivalent to, for example, impingement on an adiabatic ceiling or a saline plume impinging on the floor of a basin of relatively fresh water; in such a situation the buoyancy flux in the ceiling jet will be conserved. The flow in this case is closely related to the radial gravity current studied by Britter (1979). That study was mainly concerned with propagation of the initial front and the associated dynamics of the gravity-current head, although many of his conclusions remain relevant when considering the steady-state flow which follows. One feature emphasised by Britter (1979) is that for the radial gravity current, observations indicate that entrainment is confined to the current head, which entrains in such a manner as to regulate the Froude number (defined later) of the flow. Entrainment is negligible in the stably stratified flow that follows the head.

Ambient density, ρ: kg/m^3	1
Entrainment constant, α	0·1
Gravitational acceleration, g: m/s^2	9·81
Heat capacity of air, C_{P}: (J/kg)/K	1005
Thermal expansion coefficient, β: K^{-1}	$3{\cdot}4 \times 10^{-3}$
Function of Fr, see Equation 11, c_1	0·5

Table 1. Physical parameters used in the comparison of theory with data

Following Britter (1979), similarity considerations lead to the construction of a horizontal velocity scale u, which depends on the current buoyancy flux and the (radial) distance from the centre

3. $$u = c_1 F_{\mathrm{c}}^{1/3} r^{-1/3}$$

where F_{c} is the buoyancy flux in the ceiling current, r is the radial distance and c_1 is a dimensionless proportionality constant. Denoting the time-independent volume flux in the ceiling current by V_{c} and a depth scale for the ceiling current by h, then

4. $$V_{\mathrm{c}} = 2\pi r u h$$

and hence the current depth becomes

5. $$h = \frac{V_{\mathrm{c}}}{2\pi c_1} F_{\mathrm{c}}^{-1/3} r^{-2/3}$$

If there is no entrainment into the steady current, as observed by Britter (1979), then V_{c} is a constant and the spatial variation in the current depth scale is defined completely by the explicit radial dependence in Equation 5. It is convenient at this point to complete the ceiling-jet description with the form of the ceiling-jet reduced gravity

6. $$g'_{\mathrm{c}} = F_{\mathrm{c}}/V_{\mathrm{c}}$$

from which it may be noted that the reduced gravity is also constant in the case of no entrainment or thermal exchange.

The solution for the ceiling jet is derived from the radial gravity current by matching the buoyancy and volume fluxes

7. $$F_{\mathrm{c}} = F_{\mathrm{p}}$$

and

$$\begin{aligned} V_c &= V_p \\ &= \pi b^2 w \\ &= \pi^{2/3} \frac{6\alpha}{5} \left(\frac{9\alpha}{10}\right)^{1/3} F_p^{1/3} H^{5/3} \end{aligned} \tag{8}$$

where V_p is the volume flux in the plume. With these conditions, we obtain

$$u = c_1 F_p^{1/3} r^{-1/3} \tag{9a}$$

$$\frac{h}{H} = \frac{3\alpha}{5c_1\pi^{1/3}} \left(\frac{9\alpha}{10}\right)^{1/3} \left(\frac{r}{H}\right)^{-2/3} \tag{9b}$$

$$g'_c = \frac{5}{6\alpha\pi^{2/3}} \left(\frac{9\alpha}{10}\right)^{-1/3} F_p^{2/3} H^{-5/3} \tag{9c}$$

Several points about the impingement-current solution (Equation 9) may be noted immediately.

- Velocity u is independent of the ceiling height H.
- Current depth h, like the plume width b, is independent of the buoyancy flux F_p.
- The reduced gravity g'_c remains equal to the value attained by the plume upon impingement.

Note also that the expression for the impingement-current depth (Equation 9b) takes a simple dimensionless form, with both the depth and radial coordinate non-dimensionalised by the ceiling height H. This is because the impingement-current properties are set by the plume properties at impingement, which in turn depend on the plume evolution through the total height of rise, rather than because the current is directly affected in some manner by the enclosure dimensions.

It has been noted that the solution given by Equation 9 is not compatible with a basic version of the axisymmetric shallow-water equations for mean flow variables only, in which the static pressure head $((u^2/2) + g'_c h)$ of the current is conserved (Grundy and Rottman, 1986). There are, however, other forces not considered in that treatment, which act to remove energy from the mean flow. Examples of these include stresses at the top and bottom boundaries of the current, which have been discussed by Britter (1979) and You (1985), and vortex effects arising from the stretching of the turbulent azimuthal vorticity component, as discussed by Rooney (1997).

The solution (Equation 9) is completely specified by the plume buoyancy flux and entrainment constant, the ceiling height, the radial distance from the domain centreline and the proportionality constant c_1. The last of these is thus far unknown and requires further examination. The most obvious constraint on the impingement current is the regulation of the Froude number (Fr) at a value close to unity, noted by Britter (1979). The Froude number depends on the current properties as

$$\mathrm{Fr} = \frac{u}{(g'_c h)^{1/2}} \tag{10}$$

and hence, using Equation 9, is related to c_1 by

$$c_1 = (2\pi)^{-1/3}\mathrm{Fr}^{2/3} \approx 0{\cdot}54\mathrm{Fr}^{2/3} \tag{11}$$

Thus it is expected that c_1 is also of order unity. For example, if the extrema of the typical range of Fr are examined (Simpson, 1982), $\mathrm{Fr} = 0{\cdot}7 \Rightarrow c_1 \approx 0{\cdot}43$ and $\mathrm{Fr} = 1{\cdot}0 \Rightarrow c_1 \approx 0{\cdot}54$. A representative value of $c_1 = 0{\cdot}5$ will therefore be assumed.

2.3 Stagnation-point heat transfer

Before considering heat loss from the ceiling jet to the ceiling, heat loss in the impingement region must be considered, often referred to as stagnation-point heat transfer. Donaldson *et al.* (1971) and You and Faeth (1979) previously considered this problem, for a jet impinging on a heated surface and a fire plume impinging on a ceiling respectively. They each began with a theoretical expression for the heat flux per unit area in a laminar flow with centreline velocity v_e

$$\dot{q}_{\mathrm{lam}} = E\mathrm{Pr}^F \left[\nu\left(\frac{\partial v_e}{\partial r}\right)_{r=0}\right]^{1/2} C_P \rho \Delta T_s \tag{12}$$

where ν is the kinematic viscosity, Pr is the Prandtl number (the ratio of kinematic viscosity to thermal diffusivity), C_P and ρ are the specific heat capacity and density of air respectively and ΔT_s is the temperature difference between the impinging fluid and the ceiling. Donaldson *et al.* (1971) took $E = 2^{-1/2} \approx 0{\cdot}707$ and $F = -0{\cdot}5$ and You and Faeth (1979) took $E = 0{\cdot}763$ and $F = -0{\cdot}6$.

Extension to the turbulent case proceeds by the substitution $\partial v_e/\partial r = Aw/b$, where Donaldson *et al.* (1971) obtained $A = 1{\cdot}13$ from jet measurements. (Note that in the original notation of these papers, this coefficient is denoted by α; it has been changed to A here to avoid confusion with the entrainment constant.) Thus, Donaldson *et al.* (1971) derived a Nusselt number

$$\begin{aligned}\mathrm{Nu} &= \frac{\dot{q}_{\mathrm{lam}}}{k\Delta T_{\mathrm{s}}/b} \\ &= 2^{-1/2}A^{1/2}\mathrm{Pr}^{-1/2}\frac{\nu C_{\mathrm{P}}\rho}{k}\left(\frac{wb}{\nu}\right)^{1/2} \\ &= 2^{-1/2}A^{1/2}\mathrm{Pr}^{1/2}\mathrm{Re}^{1/2}\end{aligned} \tag{13}$$

where k is the thermal conductivity and Re ($= wb/\nu$) is the Reynolds number. This does not require modelling of w or b in terms of more fundamental experimental parameters. Donaldson *et al.* (1971) also presented results showing that the normalised actual heat flux $\dot{q}$ is an increasing function of the dimensionless distance between the jet and the impingement surface

$$\frac{\dot{q}}{\dot{q}_{\mathrm{lam}}} = \varphi\left(\frac{H}{d_{\mathrm{N}}}\right) \tag{14}$$

where d_{N} is the jet nozzle diameter. The magnitude of φ varies from approximately 1·4 (at $H/d_{\mathrm{N}} = 7$) to 2·2 (at $H/d_{\mathrm{N}} = 30$).

You and Faeth (1979), on the other hand, obtained a dimensionless heat flux using the ceiling height and the source power, assuming that ΔT_{s} is equal to the plume/ambient temperature difference ΔT

$$\begin{aligned}\frac{\dot{q}H^2}{\dot{Q}} &= 0{\cdot}763A^{1/2}\mathrm{Pr}^{-3/5}\nu^{1/2}H^2\left(\frac{w}{b}\right)^{1/2}\frac{\rho C_{\mathrm{P}}}{\beta\boldsymbol{g}\dot{Q}}\beta\boldsymbol{g}\Delta T \\ &= 0{\cdot}763A^{1/2}\mathrm{Pr}^{-3/5}\nu^{1/2}H^2F_{\mathrm{p}}^{-1}\boldsymbol{g}'_{\mathrm{p}}w^{1/2}b^{-1/2}\end{aligned} \tag{15}$$

with the definition of reduced gravity $\boldsymbol{g}'_{\mathrm{p}} = \beta\boldsymbol{g}\Delta T$. Using a plume similarity solution equivalent to Equation 1, You and Faeth (1979) obtained

$$\begin{aligned}\frac{\dot{q}H^2}{\dot{Q}} &= 0{\cdot}763\pi^{-5/6}\left(\frac{9\alpha}{10}\right)^{-1/6}\left(\frac{5}{6\alpha}\right)^2A^{1/2}\mathrm{Pr}^{-3/5}\mathrm{Ra}^{-1/6} \\ &= 0{\cdot}207\alpha^{-13/6}A^{1/2}\mathrm{Pr}^{-3/5}\mathrm{Ra}^{-1/6}\end{aligned} \tag{16}$$

where

$$\mathrm{Ra} = \frac{H^2F_{\mathrm{p}}}{\nu^3} \tag{17}$$

and the validity range is $10^9 < \mathrm{Ra} < 10^{14}$. Taking the entrainment constant $\alpha = 0{\cdot}1$ gives a value for the constant of $0{\cdot}207\alpha^{-13/6} \approx 30{\cdot}5$. You and Faeth (1979) did not use the α-based coefficients of the similarity solution (Equation 1) but instead used empirical coefficients from which they derived a value for the constant of 62·4, which is approximately double the value based on α. However, they found that they had to reduce the value of A by an approximate factor of 4, to $A = 0{\cdot}25$, in order to fit their data. Thus, the α-based value combined with the original value of A provides an equivalent satisfactory fit to the data.

It therefore appears that the use of the laminar expression for the heat flux, with the substitution of Aw/b for the laminar stagnation-point velocity gradient, is adequate for the modelling of plume heat transfer, but may underestimate jet heat transfer by a factor of up to 2·2. You and Faeth (1979) went on to state that in comparable conditions to the experiments of Donaldson *et al.* (1971) (note in particular they specified the identity of the temperature difference), they found the plume stagnation-point heat flux $\dot{q}_{\mathrm{p}}$ to the ceiling to be lower than that of the equivalent impinging jet $\dot{q}_{\mathrm{j}}$, such that $\dot{q}_{\mathrm{p}}/\dot{q}_{\mathrm{j}}$ was in the range 0·24–0·38. They were unable to account for this difference, but the success of the similarity approach in the plume case indicates that it may be extended to compare the plume and jet cases and provide a possible explanation (see the Appendix).

The stagnation-point heat loss by the flow means that the conservation of buoyancy flux (Equation 7) must be revisited. The ceiling heat flux per unit area $\dot{q}$ is equivalent to a loss of buoyancy per unit area f in the impingement region, so that, after Equation 16, it is possible to write

$$\frac{fH^2}{F_{\mathrm{p}}} = 0{\cdot}763\pi^{-5/6}\left(\frac{9\alpha}{10}\right)^{-1/6}\left(\frac{5}{6\alpha}\right)^2A^{1/2}\mathrm{Pr}^{-3/5}\mathrm{Ra}^{-1/6} \tag{18}$$

Taking the radius of the impingement region to be described approximately by the plume radius at the ceiling (Equation 1b) means that the total buoyancy loss in the impingement region is proportional to fH^2. Thus the dependence of Ra on F_{p} (Equation 17) means that the heat transfer in the impingement region, as a proportion of the convective power of the source, weakly decreases as the convective power increases, even though the total heat transfer increases. It can be speculated that this is caused by the reduced efficiency of boundary-layer processes as plume conditions become more extreme.

The difference in the initial ceiling-jet and plume buoyancy fluxes is equal to the loss of buoyancy flux in the impingement region

$$\begin{aligned}F_{\mathrm{p}} - F_{\mathrm{c}} &= \pi\left(\frac{6\alpha}{5}\right)^2H^2f \\ &= 0{\cdot}763\left(\frac{9\alpha}{10\pi}\mathrm{Ra}\right)^{-1/6}A^{1/2}\mathrm{Pr}^{-3/5}\,F_{\mathrm{p}}\end{aligned} \tag{19}$$

You and Faeth (1979) pointed out that their definition of Ra can be directly related to Re through the plume similarity solution. Using Equation 1

20. $$\mathrm{Re} = \frac{wb}{\nu} = \left(\frac{9\alpha}{10\pi}\mathrm{Ra}\right)^{1/3}$$

Hence it is possible to write

21. $$F_\mathrm{c} = F_\mathrm{p}(1 - 0{\cdot}763A^{1/2}\mathrm{Pr}^{-3/5}\mathrm{Re}^{-1/2})$$

Substituting $A = 1{\cdot}13$ and taking $\mathrm{Pr} \approx 0{\cdot}7$ for air yields a coefficient of $\mathrm{Re}^{-1/2}$ very close to unity and so

22. $$F_\mathrm{c} \approx F_\mathrm{p}(1 - \mathrm{Re}^{-1/2})$$

and the equivalent validity range is approximately $300 < \mathrm{Re} < 14\,000$. Thus, for example, a plume with a Reynolds number of 1000 at impingement would lose less than 4% of its buoyancy flux by heat transfer in the impingement region according to this analysis. For the flows to be discussed here, Re is at the upper end of the range considered, as will be shown in Section 3.2. The implication is that the conservation of buoyancy flux (Equation 7) is a reasonable approximation in the construction of a ceiling-jet similarity solution.

2.4 Ceiling-jet heat transfer

The ceiling-jet model in the diabatic case may be written as a modification of the buoyancy-conserving case

23a. $$u = c_1 F_\mathrm{p}^{1/3} r^{-1/3} f_1$$

23b. $$\frac{h}{H} = \frac{3\alpha}{5c_1\pi^{1/3}}\left(\frac{9\alpha}{10}\right)^{1/3}\left(\frac{r}{H}\right)^{-2/3} f_2$$

23c. $$\boldsymbol{g}'_\mathrm{c} = \frac{5}{6\alpha\pi^{2/3}}\left(\frac{9\alpha}{10}\right)^{-1/3} F_\mathrm{p}^{2/3} H^{-5/3} f_3$$

where f_1, f_2 and f_3 are unknown functions, which are unity in the case of zero heat transfer. It is assumed that the flow modifications arise solely from heat transfer to the ceiling and that stable stratification and lack of entrainment mean that heat transfer to the ambient may be neglected as a first approximation.

The ceiling-jet similarity solution (Equation 9) has a constant Froude number ($\mathrm{Fr} = \mathrm{Ri}^{-1/2}$). The experiments of Chobotov (1987) showed that the current Richardson number Ri maintained a value of approximately unity in a 2D thermally buoyant current, despite convective heat loss to the adjacent boundary. (The current in these experiments was also observed to exhibit negligible entrainment.) It may therefore be assumed that the property of constant Fr is maintained in the diabatic case and so, taking $\mathrm{Fr} \approx 1$,

24. $$f_1^2 \approx f_2 f_3$$

The convective heat transfer per unit area may be modelled as proportional to both the current speed and the current/ceiling temperature difference

25. $$\dot{q} = c_2 \rho C_\mathrm{P} \Delta T_\mathrm{s} u$$

where c_2 is a dimensionless constant, akin to a heat-transfer coefficient, and ΔT_s is the temperature difference between the current and the ceiling surface. The dependence on speed u has been incorporated (e.g. by You (1985)) and observed experimentally in the 2D case by Chobotov (1987), expressed as the observed linear dependence of the Nusselt number on the Reynolds number, $\mathrm{Nu} = 0{\cdot}13\mathrm{Re}$.

From Equations 23 and 25, taking $\Delta T = \Delta T_\mathrm{s}$

26. $$\begin{aligned}\frac{\mathrm{d}F_\mathrm{c}}{\mathrm{d}r} &= -2\pi r\left(\frac{\boldsymbol{g}\beta}{\rho C_\mathrm{P}}\right)\dot{q} \\ &= -2\pi c_2 r \boldsymbol{g}'_\mathrm{c} u \\ &= -c_1 c_2 \frac{5}{3\alpha}\left(\frac{9\alpha}{10\pi}\right)^{-1/3} F_\mathrm{p} r^{2/3} H^{-5/3} f_1 f_3\end{aligned}$$

or

27. $$\frac{1}{F_\mathrm{p}}\frac{\mathrm{d}F_\mathrm{c}}{\mathrm{d}\tilde{r}} = -c_1 c_2 \frac{5}{3\alpha}\left(\frac{9\alpha}{10\pi}\right)^{-1/3} \tilde{r}^{2/3} f_1 f_3$$

where $\tilde{r} = r/H$. This dimensionless coordinate was used by Alpert (1975) to correlate observations of the modification of ceiling-jet reduced gravity in the diabatic case (represented by the function f_3 above) as suggested by Heskestad (1972) and reported by Cooper (1982). It has also been used (You, 1985; You and Faeth, 1979) to correlate measurements of dimensionless ceiling-jet heat transfer of fire plumes. The implication here is that $f_i = f_i(r/H)$, $i = 1, 3$. Repeating the point made earlier, the presence of H in this solution should be interpreted as the effect of the plume evolution on the current initial conditions.

The ceiling-current velocity does not depend on the ceiling height in the adiabatic case; therefore, this may be assumed to remain true in the case of heat transfer. Thus

28. $$f_1 = 1$$

and hence

29. $$f_2 = f_3^{-1}$$

That is, the ceiling-current velocity is unchanged in the diabatic case and a constant Fr is maintained by a balance between the reduced gravity and the ceiling-current depth. The model of the diabatic ceiling current then becomes

30a. $$u = c_1 F_p^{1/3} r^{-1/3}$$

30b. $$\frac{h}{H} = \frac{3\alpha}{5c_1\pi^{1/3}}\left(\frac{9\alpha}{10}\right)^{1/3}\left(\frac{r}{H}\right)^{-2/3} f_3^{-1}$$

30c. $$\boldsymbol{g}_c' = \frac{5}{6\alpha\pi^{2/3}}\left(\frac{9\alpha}{10}\right)^{-1/3} F_p^{2/3} H^{-5/3} f_3$$

with $f_3 = f_3(r/H)$ and heat transfer governed by Equation 25.

The parameter dependencies of the solution (Equation 30) agree with previous methods of presenting fire ceiling-jet data, as summarised in the work of Motevalli and Marks (1991) where various measurements of maximum ceiling-jet velocity and temperature difference were unified using the dimensionless forms

31a. $$u^* = u_m/Q^{*1/3}(\boldsymbol{g}H)^{1/2}$$

31b. $$\Delta T^* = \Delta T_m/Q^{*2/3}T$$

which are found to be functions of (r/H) only. The dimensionless form for the convective power is

32. $$Q^* = \dot{Q}/\rho C_P T \boldsymbol{g}^{1/2} H^{5/2}$$

where ρ and T are the ambient air density and temperature respectively, C_P is as in Table 1 and the subscript m denotes maximum values. If it is assumed that $\beta \sim T^{-1}$, which is consistent with the Boussinesq approximation (and ideal gas law), then $Q^* = F_p \boldsymbol{g}^{-3/2} H^{-5/2}$ and $\boldsymbol{g}_c' = \boldsymbol{g}\Delta T/T$. If it is also assumed that the maximum and scaling values have a ratio R, so that $u_m = Ru$ and $\Delta T_m = R\Delta T$ then, from Equation 30

33a. $$u_m/Q^{*1/3}(\boldsymbol{g}H)^{1/2} = RuF_p^{-1/3}H^{1/3} = Rc_1(r/H)^{-1/3}$$

33b. $$\Delta T_m/Q^{*2/3}T = R\boldsymbol{g}_c' F_p^{-2/3} H^{5/3} = R\frac{5}{6\alpha\pi^{2/3}}\left(\frac{9\alpha}{10}\right)^{-1/3} f_3$$

Thus the solution (Equation 30) agrees with, and to some extent explains, the dimensionless scaling of ceiling-jet data observed previously (Equation 31). Motevalli and Marks (1991) also made the case for a similar scaling with (r/H) of the current depth scale, when this is normalised by H. The present solution for the current depth (Equation 30b) strengthens the argument for that scaling.

For applications at early times when $\Delta T_s = \Delta T$, the model forms of the ceiling-current temperature and heat transfer may be stated explicitly. First, for temperature, from Equation 30c

34. $$(\beta\boldsymbol{g})^{1/3}(\rho C_P)^{2/3}\frac{H^{5/3}\Delta T}{\dot{Q}^{2/3}} = \frac{5}{6\alpha\pi^{2/3}}\left(\frac{9\alpha}{10}\right)^{-1/3} f_3$$

Second for heat transfer, from Equations 25 and 30

35. $$\frac{\dot{q}H^2}{\dot{Q}} = c_1 c_2 \frac{5}{6\alpha\pi^{2/3}}\left(\frac{9\alpha}{10}\right)^{-1/3}\left(\frac{r}{H}\right)^{-1/3} f_3$$

The form of f_3 and the value of c_2 are not given by the model but may be examined by experiment.

3. Experiments

The model described in Section 2 may be verified and extended using some results from the experiments of Rooney (1997). The relevant subset of experiments is now described.

3.1 Apparatus, instrumentation and data handling

The experiments were carried out using a steel ceiling, 2·5 m in diameter and several millimetres thick, which was suspended horizontally approximately 2 m above a solid floor, within a larger enclosure consisting of a roof with fan ventilation and sides of porous curtain to minimise the effect of ambient disturbances. Four Medtherm type 64 heat-flux transducers were mounted in the ceiling. These were positioned along one radius and flush with the lower surface of the ceiling, at radial distances of 100, 380, 750 and 1100 mm from the centre. Temperature-sensing thermocouples (K-type) were suspended from the ceiling along a radius at right angles to that of the heat-flux meters, at radial distances of 430, 800 and 1060 mm from the centre. The data presented here are taken from thermocouples at a vertical displacement of 20 mm below the ceiling.

Data were collected in all experiments over an interval of 25 s (much longer than any flow-fluctuation time scales), beginning after the flow appeared to have established a steady state. Sampling rates were 2 Hz for the thermocouples and 100 Hz for the heat-flux meters, and the data were time-averaged over the recording period to give mean values. Changing the averaging window did not significantly alter these mean values.

3.2 Fire types and characterisation

Two different types of fire were used, referred to as pan and crib fires. The pan fire consisted of a shallow cylindrical metal container, 230 mm in diameter, containing 100 ml of liquid organic fuel, which burned while floating on a layer of water. The crib fire was a conventional wood crib, constructed from four layers of five red pine sticks laid alternately crosswise. These sticks were 250 mm long, of square cross-section with side 25 mm.

The power of the fires was measured directly, by weighing the pan fires continuously, and indirectly, from known correlations of power, mean flame height and source diameter (Drysdale, 1985). The fires were of similar size (horizontal dimension and flame length) and were estimated to have total power outputs of approximately 30 kW. This figure is more reliable for the pan fires on account of the weighing technique. Since 30–40% of the total power is typically lost by radiation from luminous flames (Drysdale, 1985; Tamanini, 1977), the estimated convective power was taken as approximately 20 kW. Based on Equation 2, this is equivalent to a buoyancy flux of approximately 0·66 m^4/s^3.

Radiation losses are generally split between the visible spectral range and the infrared range. The ceiling materials would be expected to have a relatively high albedo, especially at low incidence angles, which would reduce the visible absorption, and the presence of smoke both in the plume and the ceiling jet shields the ceiling from direct radiation incidence. Thus, the direct radiative effect on the ceiling will be neglected as a first approximation. The results will demonstrate the validity of this assumption, both by their adherence to power-law form and by the flux magnitudes, as well as by the manner in which the interrelation between temperature and heat-flux data accords with the theory presented earlier.

3.3 Method

The experiments involved setting fires at depths of 750, 1200 and 1700 mm below the ceiling, each configuration being labelled as indicated in Table 2. Table 2 also shows the plume Reynolds number at impingement as estimated from the buoyancy flux, using Equations 17 and 20. Simultaneous measurements of heat flux and temperature were taken during each experiment.

Fire type	Label	Ceiling height: mm	Re ($\times 10^4$)
Crib	c75	750	1·4
Crib	c12	1200	1·9
Crib	c17	1700	2·4
Pan	p75	750	1·4
Pan	p12	1200	1·9
Pan	p17	1700	2·4

Table 2. Combinations of fire types and ceiling heights used in the experiments, and the value of plume Re at impingement, based on the ceiling height and the estimated buoyancy flux

4. Results

The measurements of ceiling-jet temperature difference (from a background of approximately 290K) and ceiling heat flux in the ceiling-jet region, for all fires, are plotted in Figures 2 and 3 respectively. Both the data and the radial coordinate were scaled with the ceiling height above the fire H in accordance with the theory set out in Section 2.4. The power of the fires was not included in the scaling, although the collapse of data for both fire types validates the estimate of equal convective power. The magnitude of the heat fluxes indicates an expected ceiling temperature increase of much less than 10% by the end of an experiment. This is sufficiently small that the applicability of Equations 34 and 35 may be assumed. Lines have been fitted through the data in both figures.

Based on the fit to the temperature data, $H^{5/3}\Delta T = 46(r/H)^{-0{\cdot}8}$, comparison with Equation 34 taking parameter values as given in Table 1 yields the form of the unknown function as

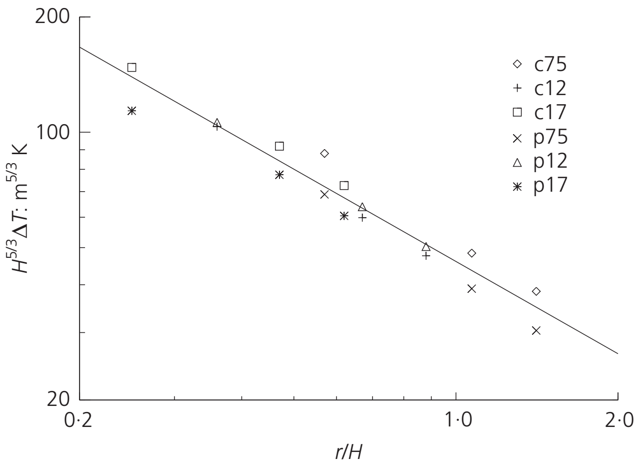

Figure 2. Ceiling-jet temperature measurements presented as a difference above the ambient temperature (~290K) and scaled using the ceiling height H. The data are labelled according to Table 2 and the line drawn on the figure has the form $H^{5/3}\Delta T = 46(r/H)^{-0{\cdot}8}$

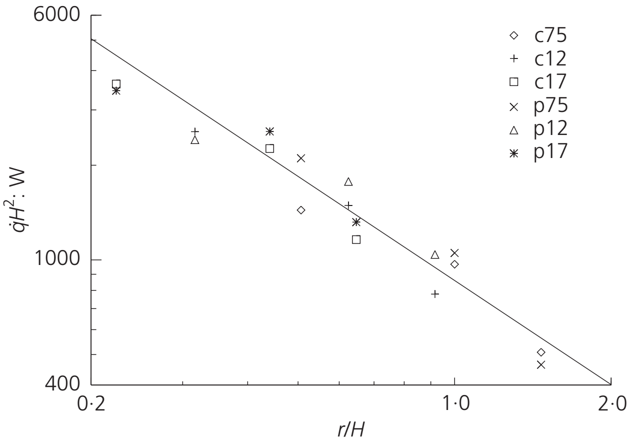

Figure 3. Heat flux measurements in the ceiling-jet region scaled using the ceiling height H. The data are labelled according to Table 2 and the line drawn on the figure has the form $\dot{q}H^2 = 860(r/H)^{-1{\cdot}1}$

36. $$f_3 = 0{\cdot}23(r/H)^{-0{\cdot}8}$$

Substituting this function in Equation 35 yields

37. $$\frac{\dot{q}H^2}{\dot{Q}} = 0{\cdot}23c_1c_2\frac{5}{6\alpha\pi^{2/3}}\left(\frac{9\alpha}{10}\right)^{-1/3}\left(\frac{r}{H}\right)^{-1{\cdot}13}$$

Comparing with experiment, first, the line through the heat-flux data, $\dot{q}H^2 = 860(r/H)^{-1{\cdot}1}$ (Figure 3), agrees satisfactorily in respect of the predicted exponent of (r/H) in Equation 37. Second, substitution of the parameter values in Equation 37 gives an estimate for the dimensionless heat-transfer coefficient of

38. $$c_2 = 0{\cdot}043$$

Referring to Equation 25, this value is equivalent to a dimensional constant of approximately 45 (J/m^3)/K in that relationship. In the 2D case, the relationship obtained by Chobotov (1987) is

39. $$\dot{q} = \frac{0{\cdot}13k}{\nu}\Delta Tu$$

where k and ν are the thermal conductivity and kinematic viscosity of the fluid, respectively. The experiments from which this result was derived were for currents of air heated to approximately 530K. Interpolating the properties of dry air given by Batchelor (1967) predicts values of k and ν at this temperature of approximately $4{\cdot}0 \times 10^{-2}$ (J/m)/s per K and $4{\cdot}3 \times 10^{-5}$ m^2/s respectively, and thus a value of the constant of approximately 120 (J/m^3)/K. The constant is of the same order in the two cases, but different by a factor of approximately 3.

A closer equivalence than this may not be expected given the differences in method and geometry between the fire plume experiments discussed here and the experiments of Chobotov (1987). For instance, observed longitudinal-roll structure within the flow in the 2D case is aligned with the flow (Chobotov, 1987), whereas coherent structures in the axisymmetric case tend to take the form of arcs or circles transverse to the flow. Despite such differences, the agreement in magnitude between the cases is encouraging.

5. Conclusion

A theoretical model of plume impingement on a surface has been presented. The model has considered isothermal flow, as well as heat transfer to the surface both in the impingement and ceiling-jet regions, in the case of a thermally buoyant plume.

It has been shown that, for turbulent flows, the loss of heat in the impingement region as a proportion of the source strength is predicted to decrease as the source strength increases. It has also been shown that modelling the ceiling current as a radial gravity current without significant entrainment (except in the current head) and with Froude number similarity produces a ceiling-jet model with the scaling of flow properties often exploited in studies of impinging fire plumes.

A model of heat transfer in the ceiling-jet region, which incorporates a dependence on the impingement-current velocity scale, was found to agree with experimental results. This dependence also accounts for the differing radial evolution of current temperature and heat transfer.

Appendix: Comparing plume and jet stagnation-point heat transfer

First, briefly recall the derivation of the jet similarity solution. The evolution equations for a narrow, axisymmetric turbulent flow, such as a plume or jet, are (Turner, 1973)

40a. $$\frac{d}{dz}(b^2w) = 2\alpha bw$$

40b. $$\frac{d}{dz}(b^2w^2) = b^2\boldsymbol{g}'_p$$

40c. $$\frac{d}{dz}(b^2w\boldsymbol{g}'_p) = -b^2wN^2$$

where

41. $$N^2 = -\frac{\boldsymbol{g}}{\rho_1}\frac{\mathrm{d}\rho}{\mathrm{d}z}$$

is the squared buoyancy frequency of the environment with density profile $\rho(z)$ depending on the vertical coordinate z and the reference density $\rho_1 = \rho(0)$.

The pure-plume similarity solution of Equation 40, at height $z = H$, is given in Equation 1. In the case of a source and ambient of the same uniform density, Equations 40 simplify greatly and the similarity solution for a non-buoyant jet may be derived as

42a. $$w = \frac{1}{2\alpha\pi^{1/2}}M^{1/2}z^{-1}$$

42b. $$b = 2\alpha z$$

where the momentum flux $M = \pi b^2 w^2$ is now constant.

For the same temperature difference at the ceiling (and neglecting differences in ρ), the ratio of plume and jet heat fluxes reduces to

43. $$\frac{\dot{q}_\mathrm{p}}{\dot{q}_\mathrm{j}} = \left(\frac{(w/b)_\mathrm{p}}{(w/b)_\mathrm{j}}\right)^{1/2}\varphi^{-1} = \frac{5}{3}\pi^{1/12}\left(\frac{9\alpha}{10}\right)^{1/6}F_\mathrm{p}^{1/6}M^{-1/4}H^{1/3}\varphi^{-1}$$

where φ is the jet enhancement factor (Equation 14). This expression for the heat-flux ratio indicates that it increases as F increases and decreases as M increases, as might be expected, but otherwise it is difficult to interpret. To further decompose the characteristics of the flows, it is noted that, first, conservation of M in the jet means it is possible to substitute $M = \pi b_0^2 w_0^2$, where subscript 0 indicates source conditions. Second, since the temperature difference at the ceiling is the same in the two cases, it is possible to include this parameter more explicitly by substituting for F_p from the expression for reduced gravity (Equation 1c). This yields

44. $$\frac{\dot{q}_\mathrm{p}}{\dot{q}_\mathrm{j}} = \frac{5}{3}\left(\frac{27}{25}\right)^{1/4}\alpha^{1/2}\varphi^{-1}\left(\frac{H}{b_0}\right)^{1/2}\left(\frac{\boldsymbol{g}'_\mathrm{p}H}{w_0^2}\right)^{1/4}$$

Expressed in this way it may be seen that, for equivalence of plume and jet flows, it is not sufficient for the temperature difference ΔT and the ratio of domain height to source length scale (φ and H/b_0) to be controlled. The source velocity scale of the jet w_0 must also be compared to the free-fall velocity scale based on the temperature difference at the ceiling $(\boldsymbol{g}'_\mathrm{p}H)^{1/2}$. It is possible that lack of control of this aspect led to the unexplained variation of the plume/jet heat transfer ratio reported by You and Faeth (1979).

For completeness, the general case of the buoyant jet may be considered; this involves similar analysis to that presented so far. For a (vertical) buoyant jet issuing from a source of both momentum and buoyancy, the flow asymptotes to jet-like behaviour near the source and plume-like behaviour at large elevations. The length scale of the transition is determined by the jet length (Papanicolaou and List, 1988)

45. $$l_\mathrm{M} = M_0^{3/4}F_0^{-1/2}$$

where M_0 and F_0 denote the source fluxes of momentum and buoyancy respectively. Omitting φ, the appropriate factor in the heat-flux equation for a buoyant jet may be written

46. $$\left(\frac{w}{b}\right)^{1/2} = \frac{1}{2\alpha}\pi^{-1/4}M_0^{1/4}H^{-1}f_4\left(\frac{H}{l_\mathrm{M}}\right)$$

where

47. $$f_4\left(\frac{H}{l_\mathrm{M}}\right) \to \begin{cases} \frac{5}{3}\pi^{1/12}\left(\frac{9\alpha}{10}\right)^{1/6}\left(\frac{H}{l_\mathrm{M}}\right)^{1/3} & \text{for } \left(\frac{H}{l_\mathrm{M}}\right) \gg 1 \\ 1 & \text{for } \left(\frac{H}{l_\mathrm{M}}\right) \ll 1 \end{cases}$$

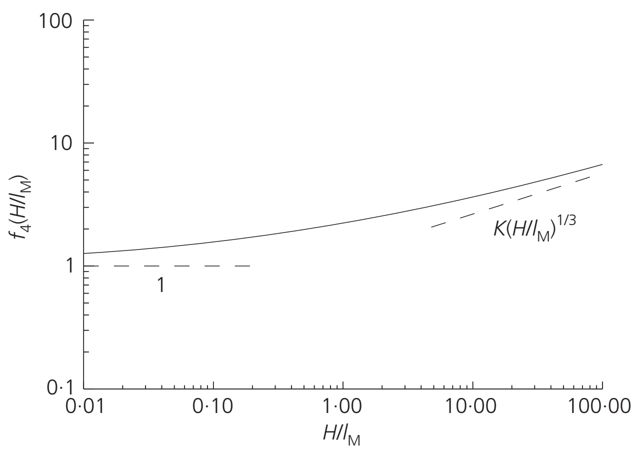

Figure 4. Sketch of the function with the limiting behaviour described in Equation 47 where $K = (5/3)\pi^{1/12}(9\alpha/10)^{1/6}$. The curve shown was generated by adding the two limiting forms (dashed lines)

The form of $f_4(H/l_M)$ is otherwise not specified, but it may be represented adequately by a sum of these limits (Figure 4).

It is evident that, for instance, the jet length marks a transition in the scaling of the stagnation-point heat flux of a vertical buoyant jet. For given source conditions, as H is increased, the heat transfer makes a transition from H^{-1} scaling to $H^{-2/3}$ scaling at $H \sim l_M$.

Acknowledgements

Thanks are due to Stuart Jagger and Graham Atkinson for their support of this project. The provision of technical facilities and financial support by the UK Health and Safety Executive is also gratefully acknowledged.

REFERENCES

Alpert RL (1975) Turbulent ceiling-jet induced by large-scale fires. *Combustion Science and Technology* **11**: 197–213.
Batchelor GK (1967) *An Introduction to Fluid Dynamics*. Cambridge University Press, Cambridge, UK.
Beyler CL (1986) Fire plumes and ceiling jets. *Fire Safety Journal* **11**: 53–75.
Britter RE (1979) The spread of a negatively buoyant plume in a calm environment. *Atmospheric Environment* **13**: 1241–1247.
Carling JC and Hunt BL (1974) The near wall jet of a normally impinging, uniform, axisymmetric, supersonic jet. *Journal of Fluid Mechanics* **66**: 159–176.
Chobotov MV (1987) *Gravity Currents with Heat Transfer Effects*. PhD thesis, California Institute of Technology, Pasadena, CA, USA.
Cooper LY (1982) Heat transfer from a buoyant plume to an unconfined ceiling. *ASME Journal of Heat Transfer* **104**: 446–451.
Devenish BJ, Rooney GG and Thomson DJ (2010) Large-eddy simulation of a buoyant plume in uniform and stably stratified environments. *Journal of Fluid Mechanics* **652**: 75–103.
Donaldson C duP, Snedeker RS and Margolis DP (1971) A study of free jet impingement. Part 2. Free jet turbulent structure and impingement heat transfer. *Journal of Fluid Mechanics* **45**: 477–512.
Drysdale D (1985) *An Introduction to Fire Dynamics*. Wiley, Chichester, UK.
Emmons HW (1991) The ceiling jet in fires. *Fire Safety Science* **3**: 249–260.
Grundy RE and Rottman JW (1986) Self-similar solutions of the shallow-water equations representing gravity currents with variable inflow. *Journal of Fluid Mechanics* **169**: 337–351.
Heskestad G (1972) Similarity relations for the initial convective flow generated by fire. *ASME Winter Annual Meeting*. ASME, New York, NY, USA, Paper 72-WA/HT-17.
Hunt GR and Linden PF (2001) Steady-state flows in an enclosure ventilated by buoyancy forces assisted by wind. *Journal of Fluid Mechanics* **426**: 355–386.
Kataoka K, Sahara R, Ase H and Harada T (1987) Role of large-scale coherent structures in impinging jet heat transfer. *Journal of Chemical Engineering of Japan* **20**: 71–76.
Motevalli V and Marks CH (1991) Characterizing the unconfined ceiling jet under steady-state conditions: A reassessment. *Fire Safety Science* **3**: 301–312.
Papanicolaou PN and List EJ (1988) Investigations of round vertical turbulent buoyant jets. *Journal of Fluid Mechanics* **195**: 341–391.
Rooney GG (1997) *Buoyant Flows from Fires in Enclosures*. PhD thesis, University of Cambridge, Cambridge, UK.
Simpson JE (1982) Gravity currents in the laboratory, atmosphere, and ocean. *Annual Review of Fluid Mechanics* **14**: 213–234.
Stevens J and Webb BW (1991) The effect of inclination on local heat transfer under an axisymmetric, free liquid jet. *International Journal of Heat and Mass Transfer* **34**: 1227–1236.
Tamanini F (1977) Reaction rates, air entrainment and radiation in turbulent fire plumes. *Combustion and Flame* **30**: 85–101.
Turner JS (1973) *Buoyancy Effects in Fluids*. Cambridge University Press, Cambridge, UK.
Watson EJ (1964) The radial spread of a liquid jet over a horizontal plane. *Journal of Fluid Mechanics* **20**: 481–499.
Yao X and Marshall AW (2007) Quantitative salt-water modeling of fire-induced flows for convective heat transfer model development. *Journal of Heat Transfer* **129**: 1373–1383.
You HZ (1985) An investigation of fire-plume impingement on a horizontal ceiling. 2: Impingement and ceiling-jet regions. *Fire and Materials* **9**: 46–56.
You HZ and Faeth GM (1979) Ceiling heat transfer during fire plume and fire impingement. *Fire and Materials* **3**: 140–147.